the zero-point levels of the two spin states. The quadrapole splitting is composed of the sum of ΔE_{val} and ΔE_{lat}; the subscript "val" refers to the contribution from the charge distribution of the aspherical "3d-valence" electron and the subscript "lat" from the charge distribution of the neighboring ions in the crystalline lattice. If the component of ΔE_{lat} in the ^6A state is assumed to be the same as that in the ^2T state in this calculation, the parameters are obtained as shown in Table III. Figures 11 and 12 show the plots of the experimental data of the quadrupole splitting together with the theoretical curves that are obtained by using the best parameters listed in Table III. These values evaluated from the TQS by the least-squares method are reliable rather than those from the temperature dependence of the effective magnetic moment, because we have neglected the distortion of the crystal field in the process of calculating the theoretical temperature dependence of the effective magnetic moment. However, not much significance is attached to this value, because there is a fair latitude in the choice of C; that is, C is defined to be constant in this calculation in spite of the fact that C may be in general dependent on temperature.

The ligand field parameters and crossover parameters for the rapid electronic relaxation of the spin-crossover system calculated in this study are similar to those for the slow electronic relaxation. The rates of $^2T \rightleftarrows {}^6A$ spin interconversion take place as fast as 10^{-7} s, although these electron transfer accompanied by changes in spin multiplicity, therefore, are spin-forbidden transitions ($\Delta s = 2$). The electron transfer must proceed through the ligand orbitals, and the interaction of an iron atom with lattice vibrations will play an important role. Furthermore, it is important that π-conjugation is involved in the chemical structure and the ligand is stereochemically flexible.

Conclusion

The Mössbauer absorption spectra for the spin-crossover iron(III) complexes showed the rapid electronic relaxation phenomena between ^6A and ^2T states. It is notable that the behavior of $[Fe(acen)(lut)_2](BPh_4)$ is different from that of the other complexes in the electronic relaxation time in spite of its similar thermodynamic data. The introduction of a methyl group in the 2-position of pyridine results in steric hindrance, leading to the inhibition of the ligand molecule motion, and changes the electron density at the iron atom. The steric hindrance affects the coupling between the spin transition and lattice vibration and thus may cause the different electronic relaxation time according to the stereochemical structure of each complex.

Registry No. $[Fe(acen)(dpp)](BPh_4)$, 83555-99-1; $[Fe(acen)(pic)_2](BPh_4)$, 62660-72-4; $[Fe(acen)(lut)_2](BPh_4)$, 86507-81-5.

Contribution from the Department of Chemistry, University of Texas, Austin, Texas 78712

Electrochemistry in Liquid Sulfur Dioxide. 4. Electrochemical Production of Highly Oxidized Forms of Ferrocene, Decamethylferrocene, and Iron Bis(tris(1-pyrazolyl)borate)[1]

PAUL R. SHARP[2] and ALLEN J. BARD*

Received November 17, 1982

The electrochemistry of $Fe(C_5H_5)_2^+$, $Fe(C_5Me_5)_2^+$, and $Fe(HB(pz)_3)_2^+$ (pz = pyrazolyl) in liquid SO_2 was investigated. All three species show one oxidation wave and one reduction wave corresponding to production of the 2+ and neutral forms, respectively. While $Fe(C_5H_5)_2^+$ is stable in SO_2, the 2+ form reacts to block the electrode surface. For $Fe(C_5Me_5)_2$ and $Fe(HB(pz)_3)_2$ both the 1+ and 2+ forms are stable on the coulometric time scale. The neutral forms react with the solvent to generate the 1+ forms. Electrochemical data and visible absorption spectra, for $Fe(C_5Me_5)_2^{2+}$ and $Fe(HB(pz)_3)_2^{2+}$, and magnetic susceptibility results, for $Fe(C_5Me_5)_2^{2+}$, are reported.

Introduction

In a previous paper we showed that liquid SO_2 is a useful solvent for the generation and study of highly oxidized transition-metal complexes.[1] In this paper we report the first observation of the two-electron-oxidation product of ferrocene, $Fe(C_5H_5)_2^{2+}$ (**1**), electrochemically generated in SO_2. In addition, stable solutions of the permethylated analogue, $Fe(C_5Me_5)_2^{2+}$ (**2**), and the related pyrazolyl borate complex $Fe(HB(pz)_3)_2^{2+}$ (**3**) have been obtained and characterized. While electrochemical oxidation of $Fe(C_5Me_5)_2$ to the 2+ form in $AlCl_3$/1-butylpyridinium chloride melts has been reported previously, under similar conditions $Fe(C_5H_5)_2^+$ was oxidized in a multiple-electron irreversible process.[3] The 2+ form of $Fe(HB(pz)_3)_2$ has not been previously reported. Our electrochemical studies suggest a closer relation (at least electronically) of the $HB(pz)_3$ ligand with the C_5Me_5 ligand rather than the previously proposed analogy with the unsubstituted C_5H_5 ligand.[4]

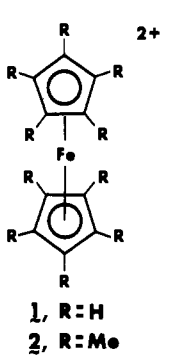

1, R = H
2, R = Me

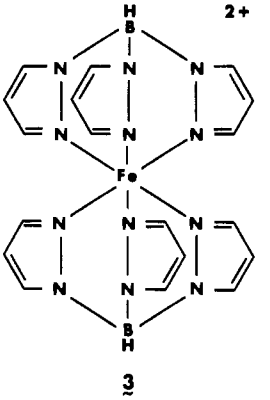

3

Experimental Section

Electrochemical studies were performed in conventional single- and three-compartment cells by using previously reported procedures.[1,5]

(1) For part 3 in this series see: Gaudiello, J. G.; Sharp, P. R.; Bard A. J. *J. Am. Chem. Soc.* **1982**, *104*, 6373–6377.
(2) Present address: Department of Chemistry, University of Missouri at Columbia, Columbia, MO 65211.
(3) Gale, R. J.; Singh, P. *J. Organomet. Chem.* **1980**, *199*, C44–C46.
(4) Trofimenko, S. *J. Am. Chem. Soc.* **1967**, *89*, 3904–3905.

0020-1669/83/1322-2689$01.50/0

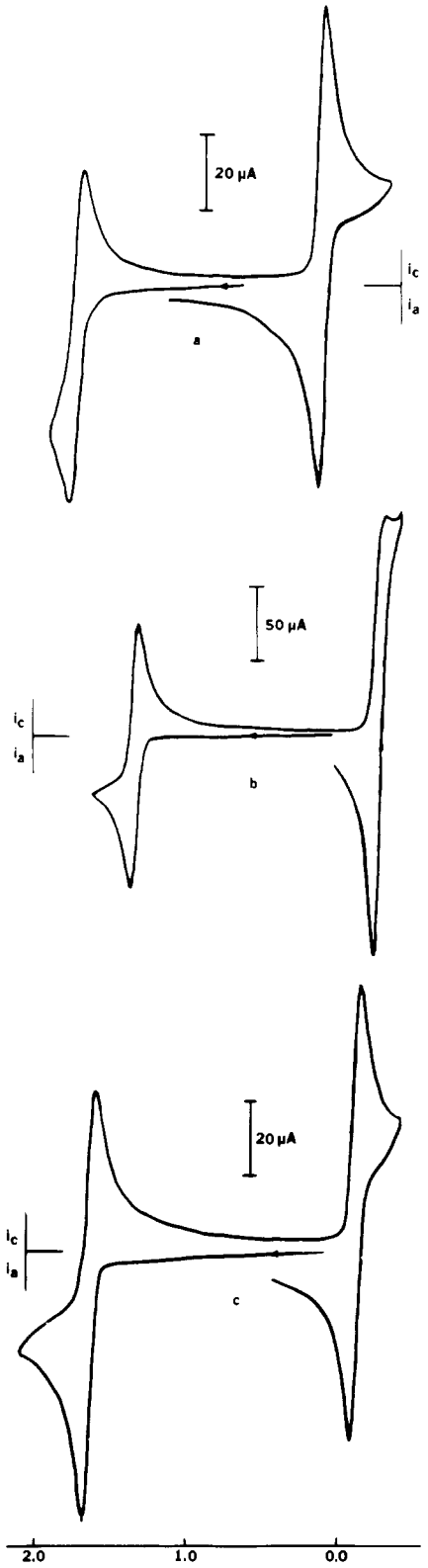

Figure 1. Cyclic voltammograms at a Pt-disk electrode (0.024 cm^2) in liquid SO_2 (−40 °C; scan rate 200 mV s^{-1}; 0.1 M $(TBA)PF_6$): (a) $Fe(C_5H_5)_2^+$, 7.5 mM; (b) $Fe(C_5Me_5)_2^+$, 10.2 mM; (c) $Fe(HB(pz)_3)_2^+$, 9.2 mM.

Scan rates employed were from 50 to 500 mV/s. All potentials are reported against a Ag quasi-reference electrode (AgRE) of a type previously described.[5] However, since some variability of this electrode was encountered, an internal reference of $Fe(bpy)_3^{2+}$ ($E^{\circ\prime}$ = 0.74 V vs. AgRE for the 2+/3+ couple in SO_2)[1] was used to confirm all potentials.

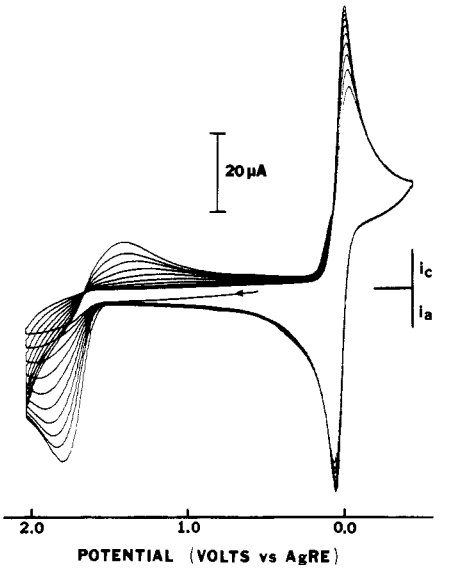

Figure 2. Scans 1–14 of a repetitive-scan cyclic voltammogram of $Fe(C_5H_5)_2^+$ in liquid SO_2 (−40 °C; scan rate 200 mV s^{-1}; 0.1 M $(TBA)PF_6$).

The magnetic susceptibility measurement, by the Evans method,[6] was made on a Nicolet NT200 superconducting instrument. The shape factor[7] for the superconducting field arrangement was substituted for that of an ordinary magnetic field arrangement used in the original equation developed by Evans.

Spectrophotometric measurements on a Cary Model 14 spectrophotometer were made with use of a vacuum-jacketed quartz cell (1-cm path length) of a design described elsewhere.[8] The solution temperature was ca. −20 °C.

Tetra-*n*-butylammonium hexafluorophosphate[1] ($(TBA)PF_6$) and $Fe(HB(pz)_3)_2$[9] were prepared as previously described. Ferrocene (Alfa) and decamethylferrocene (Strem) were used as received. $Fe(C_5Me_5)_2^+PF_6^-$ was prepared by I_2 (0.5 equiv) oxidation of $Fe(C_5Me_5)_2$ in acetone followed by the addition of a slight excess of NH_4PF_6. NH_4I was removed by filtration, and water was added. The green precipitate of $Fe(C_5Me_5)_2^+PF_6^-$ was removed by filtration, washed with water followed by dimethoxyethane and ether, and finally dried in vacuo. A solution of the product was tested for residual I^- by the addition of Ag^+(aq), with a white precipitate of AgI indicating the need for additional recrystallization (acetone/ether).

$Fe(HB)pz)_3)_2^+PF_6^-$ was prepared by an analogous procedure; however, 1.5 equiv of I_2 was required for complete oxidation, and multiple recrystallizations (acetone/ether) were needed to remove completely all traces of I_3^-.

Results

$Fe(C_5H_5)_2^+$. The cyclic voltammogram (CV) of an electroregenerated 7.5 mM SO_2 solution (−40 °C) of $Fe(C_5H_5)_2^+$ at a Pt-disk electrode is shown in Figure 1a. The reduction wave with a cathodic peak potential (E_{pc}) of 0.08 V corresponds to the Nernstian, one-electron, electrochemically reversible reduction to $Fe(C_5H_5)_2$. The difference between the anodic and cathodic peak potentials ($\Delta E_p = E_{pa} - E_{pc}$) of 48 mV corresponds closely to that expected (44 mV) for a Nernstian couple at −40 °C. The oxidation wave (E_{pa} = 1.79 V) shown in Figure 1a corresponds to a one-electron oxidation of $Fe(C_5H_5)_2^+$ to $Fe(C_5H_5)_2^{2+}$. However, only on the first scan is a reasonably clear wave observed. The effect of repetitive scanning is shown in Figure 2. $Fe(C_5H_5)_2^{2+}$ must be unstable.

(5) Tinker, L. A.; Bard, A. J. *J. Am. Chem. Soc.* **1979**, *101*, 2316–2319.

(6) Evans, D. F. *J. Chem. Soc.* **1959**, 2003–2005.
(7) Martin, M. L.; Delpuech, J. J.; Martin, G. J. "Practial NMR Spectroscopy"; Heyden and Son, Ltd: Philadelphia, PA, 1980; p 177.
(8) Gaudiello, J. G.; Bradley, P. G.; Norton, K. A.; Woodruff, W. H.; Bard, A. J. *Inorg. Chem.*, in press.
(9) Trofimenko, S. *J. Am. Chem. Soc.* **1967**, *89*, 3170–3177.

Table I. Summary of Voltammetric Parameters for the Oxidation and Reduction of $Fe(C_5H_5)_2^+$, $Fe(C_5Me_5)_2^+$, and $Fe(HB(pz)_3)_2^+$ in Liquid Sulfur Dioxide[a]

diagnostic parameter	$Fe(C_5H_5)_2^+$		$Fe(C_5Me_5)_2^+$		$Fe(HB(pz)_3)_2^+$	
	redn wave	oxidn wave	redn wave[b]	oxidn wave	redn wave	oxidn wave
E_{pa} or E_{pc}, V vs. AgRE	0.08	1.79	−0.27	1.31	−0.15	1.65
ΔE_p, mV	48	100	~50	48	48	49
$i_{pa}(i_{pc})^{-1}$ or $i_{pc}(i_{pa})^{-1}$	1	0.8	~1	1	1	1
$i_p v^{-1/2} C^{-1}$, $\mu A\ s^{1/2}\ V^{-1/2}\ mM^{-1}$	47	36	~17	49	39	38
diffusion coeff, $cm^2\ s^{-1}$	8.9×10^{-6}[c]		9.8×10^{-6}[d]		6.1×10^{-6}[d]	

[a] 0.1 M $(TBA)PF_6$; $T = -40$ °C; Pt working electrode area 0.023 cm^2. [b] $T = -30$ °C; Pt working electrode area 0.017 cm^2. [c] From reduction wave. [d] From oxidation wave.

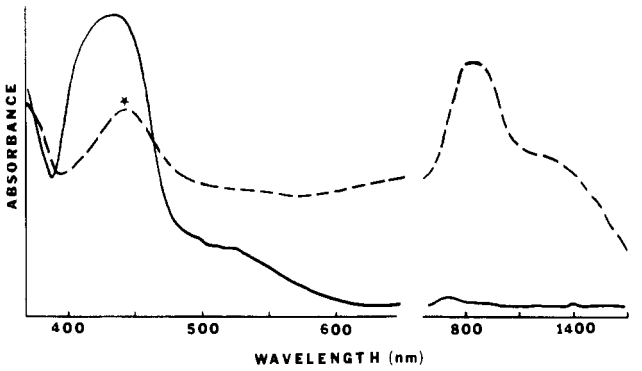

Figure 3. Absorption spectra in liquid SO_2 at ca. −20 °C of (---) $Fe(HB(pz)_3)_2^{2+}$ ($\epsilon_{max} \geq 10^4$; * = $Fe(HB(pz)_3)_2^+$) and (—) $Fe(C_5Me_5)_2^{2+}$ ($\epsilon_{max} \approx 2 \times 10^3$).

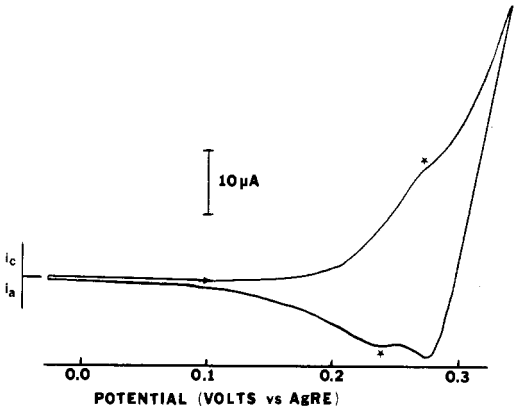

Figure 4. Cyclic voltammogram of 6.4 mM $Fe(C_5Me_5)_2^+$ at slower scan rate (20 mV s^{-1}) and increased temperature (−30 °C) (* = $Fe(C_5Me_5)_2^{1+/0}$ couple).

The decomposition product must produce a film on the electrode surface that partially blocks the electrode reactions at potentials of the 1+/2+ wave. Decomposition of the 2+ form is apparent even on the first scan, since for the 1+/2+ couple the anodic peak current, i_{pa}, for the oxidation wave is only 80% of the cathodic peak current, i_{pc}, for the 1+/0 reduction wave. The electrode surface could be partially regenerated by pulsing into the cathodic background. Similar behavior was observed when a glassy-carbon electrode was used. Essentially identical waves were observed, when neutral $Fe(C_5H_5)_2$ was the starting material. The cyclic voltammetric results are summarized in Table I.

$Fe(C_5Me_5)_2^+$. The CV of a 10.2 mM SO_2 solution of $Fe(C_5Me_5)_2^+$ at a Pt-disk electrode is shown in Figure 1b. The oxidation wave at $E_{pa} = 1.34$ V is analogous to the oxidation wave of $Fe(C_5H_5)_2^+$, but the process now corresponds to a Nernstian, one-electron, electrochemically reversible process without any decomposition or filming of the electrode surface.

Controlled-potential coulometry (CPC) of the above $Fe(C_5Me_5)_2^+$ solution at 1.6 V gave an n_{app} (faradays/mol of reactant consumed) of 0.98, confirming the one-electron nature of the oxidation. The absorption spectrum of a diluted sample of the resulting yellow-brown solution of $Fe(C_5Me_5)_2^{2+}$ is shown in Figure 3 ($\epsilon_{max} \approx 2 \times 10^3$). The solution is stable for at least 4 h at −30 °C. However, at the boiling point of SO_2 slow decomposition to the 1+ form was detected by visible spectroscopy.

For the magnetic susceptibility measurement, a 14.4 mM solution was prepared as above and a small amount of benzene was added. No reaction with the C_6H_6 occurs, as shown by cyclic voltammetry. An aliquot of this solution was transferred at −40 °C to a ^1H NMR tube containing a capillary tube filled with a mixture of SO_2 and C_6H_6 in the same proportion as the sample solution. The frequency difference between the sample and capillary C_6H_6 signals was 52 Hz at −40 °C. This gives a μ_{eff} of 2.73 μ_B, consistent with a high-spin, two-unpaired-electron configuration. The paramagnetic dication could be isolated as a gray mixture with the supporting electrolyte by removing the SO_2 in vacuo at −30 °C. This mixture was stable for at least 1 h at 25 °C in vacuo or under N_2 as shown by cyclic voltammetry after refilling the cell. Unfortunately, separation of the dication from the supporting electrolyte could not be achieved; solvents (MeCN, CH_2Cl_2, THF, dimethoxyethane) that might be used to extract the supporting electrolyte or solvent impurities decomposed the complex.

The reduction wave for $Fe(C_5Me_5)^+$ ($E_{pc} = -0.37$ V) shown in Figure 1b corresponds to the formation of neutral $Fe(C_5Me_5)_2$. However, the wave is at the edge of the cathodic background for SO_2 reduction at Pt so that both the SO_2 and the $Fe(C_5Me_5)^+$ reductions contribute to the current. Similarly, the return oxidation wave for $Fe(C_5Me_5)_2$ also overlaps with the return oxidation wave for the reduced SO_2. The reduction of SO_2 is quasi-reversible at a Pt electrode under these conditions. Resolution of the two processes can be achieved by increasing the temperature and decreasing the scan rate to the point where the solvent reduction is nearly reversible. Such a scan is shown in Figure 4, and the $Fe(C_5Me_5)^{1+/0}$ couple can now be clearly resolved at a potential more positive than that of the solvent background process. Because the potential of the $Fe(C_5Me_5)_2^{1+/0}$ couple is very near that for the SO_2 reduction process, the concentration of SO_2 is large and the bulk reduced SO_2 undergoes an irreversible coupling reaction,[10] oxidation of neutral $Fe(C_5Me_5)_2$ by SO_2 (neat) should occur. Indeed a 4.4 mM solution of $Fe(C_5Me_5)_2$ in SO_2 gives a CV essentially identical with that of the 1+ form. Only small residual currents positive of the 1+/0 couple were found, and CPC at 1 V gave a green solution of $Fe(C_5Me_5)_2^+$ with an n_{app} of only 0.24. The irreversible reactions of the reduced solvent on a coulometric time scale are indicated by the fact that the primary solvent reduction products are no longer present to be reoxidized at the electrode after electrolyis. These reaction products interfere with the oxidation of the $Fe(C_5Me_5)_2^+$, probably via reaction with $Fe(C_5Me_5)_2^{2+}$ to film the electrode, since attempted CPC at potentials sufficient to

(10) Castellonese, P.; Lacaze, P. C. *C. R. Hebd. Seances Acad. Sci., Ser. C* **1974**, *274C*, 2050–2052.

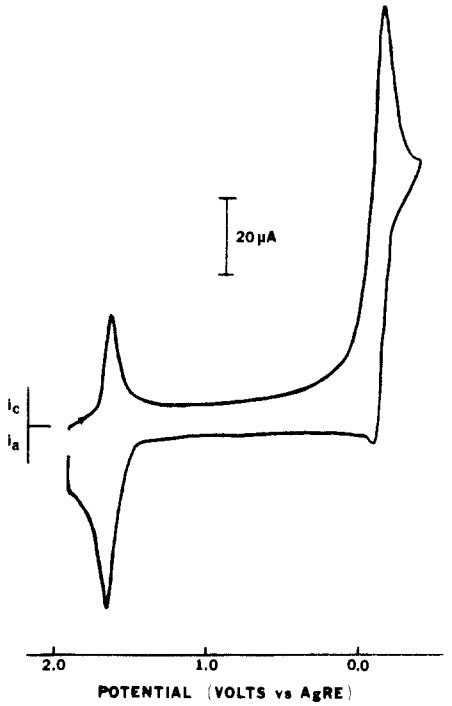

Figure 5. Cylic voltammogram of an electrogenerated 9.2 mM Fe$(HB(pz)_3)_2^{2+}$ solution (−40 °C; scan rate 200 mV s^{-1}; 0.1 M $(TBA)PF_6$).

generate the 2+ form gave initial high currents that fell rapidly to nearly zero values in seconds. This contrasts to the clean CPC oxidation found when a solution of fresh $Fe(C_5Me_5)_2^+$ was oxidized.

$Fe(HB(pz)_3)_2^+$. The cyclic voltammogram of a 9.2 mM solution of $Fe(HB(pz)_3)_2^+$ at a Pt-disk electrode is shown in Figure 1c. Although the cyclic voltammogram is almost identical with that of $Fe(C_5Me_5)_2^+$, the reduction wave at E_{pc} = −0.15 V is now sufficiently positive of the SO_2 background oxidation that no overlap occurs. The reduction wave clearly corresponds to a Nernstian, one-electron, electrochemically reversible process (ΔE_p = 48 mV). However, some bulk-solution oxidation of neutral $Fe(HB(pz)_3)_2$ by SO_2 occurs, since CPC oxidation of a 4.1 mM solution of $Fe(HB(pz)_3)_2$ at 1V and −40 °C produced a solution of the 1+ form and yielded an n_{app} value of only 0.56. Again, partial oxidation by SO_2 is predicted on the basis of the potential and concentrations. As with $Fe(C_5Me_5)_2$, the oxidation of $Fe(HB(pz)_3)_2$ by SO_2 produces products that prevent controlled-potential coulometric production of the 2+ form from solutions prepared from the neutral species.

The oxidation wave for $Fe(HB(pz)_3)_2^+$ at E_{pa} = 1.68 V shown in Figure 1c corresponds to a Nernstian, one-electron, process. CPC of the above 9.2 mM $Fe(HB(pz)_3)_2^+$ solution at 2 V gave n_{app} = 0.99. A CV of the resulting solution is shown in Figure 5. Although the waves are close to the potentials expected from the 1+ solutions, their shapes and intensities are not those for simple diffusion-controlled processes. Instead, the shape of the first reduction wave and return oxidation wave is characteristic of a surface-confined species;[11] ΔE_p is nearly zero and the peak half-widths are about 100 mV (close to the 0 and 70 mV values expected for a surface-confined species at −40 °C). The nature of the surface species is not known, although the similarity of the redox potentials to those of the solution species suggest a closely related structure. If the surface reduction wave at 1.64 V involves one electron per center and each center has a diameter

(11) Bard, A. J.; Faulkner, L. R. "Electrochemical Methods"; Wiley: New York, 1980; Chapter 12.

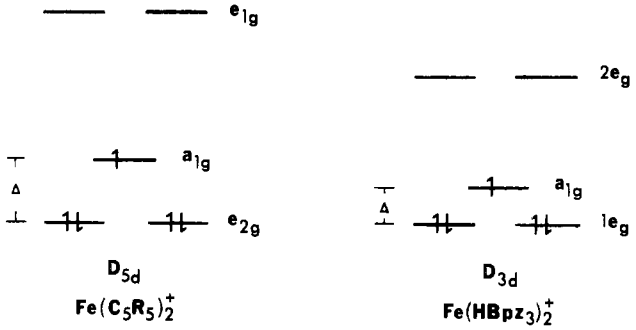

Figure 6. d-Orbital energy diagram for D_{5d} $Fe(C_5R_5)_2$ and D_{3d} $Fe(HB(pz)_3)_2$.

of 2 nm, a coverage of ca. 120 monolayers is calculated from the area under the wave.

Interestingly, no reduction of solution species (i.e., the 2+ form) occurs until the potential of the 1+/0 couple is reached, where a diffusional solution wave is observed. Surprisingly, a large Pt-gauze electrode does not seem to be similarly filmed, since the 2+ form is reduced back to the original $Fe(HB(pz)_3)_2^+$ in a CPC experiment at the expected potentials (n_{app} = 0.97 at 1 V).[12] The CV of the reduced solution showed poorly defined broad waves. By pulsing into the cathodic background, we could obtain a CV resembling that of the original $Fe(HB(pz)_3)_2^+$ solution, but with broader waves. Thus, $Fe(HB(pz)_3)_2^{2+}$ is stable on the CPC time scale (4 h) at −40 °C but must slowly lead to the formation of a film or layer on the electrode.

The absorption spectrum of the 2+ form is shown in Figure 3. Only a lower limit for the maximum extinction coefficient ($\sim 10^4$) in the range of wavelengths could be obtained because of extensive decomposition of the complex to the 1+ form at the temperature of the cell (−20 °C). Isolation of the 2+ form was not possible even as a mixture with the supporting electrolyte. A dark red product containing mostly the 1+ form was always obtained. Unfortunately, the magnetic susceptibility of the 2+ form could not be measured, because the complex reacts with the C_6H_6 used as a reference standard.

Discussion

The standard potentials and other data for the couples are listed in Table I. The effect of the electron-donating methyl groups in the $Fe(C_5R_5)_2$ pair is evident both in the negative shift of the peak potentials of the 0/1+ and 1+/2+ couples and the increased stability of the 2+ form upon methyl substitution. This effect has previously been observed for the 0/1+ couple in the Fe[3,13] as well as the Cr, Co, and Ni[13] metallocenes. $Fe(C_5H_5)_2^{2+}$ has not been previously observed. Oxidation of $Fe(C_5H_5)_2^+$ in $AlCl_3$/1-butylpyridinium chloride melts under the same conditions where $Fe(C_5Me_5)_2^{2+}$ was observed gave only a multiple-electron irreversible wave.[3]

The similarities in the electronic and coordination properties of the $HB(pz)_3$ and C_5H_5 ligand have been noted,[4] as has an increased thermal and chemical stability of $HB(pz)_3$ complexes over analogous C_5H_5 complexes. Similarily, C_5Me_5 complexes are more stable than the C_5H_5 analogues.[14] This suggests that the $HB(pz)_3$ ligand is more closely related to the C_5Me_5 ligand than to the C_5H_5 ligand. Consistent with this, the

(12) This difference in behavior between the Pt-disk and -gauze electrodes may be a result of the different pretreatments of the two electrodes. The disk electrode was cycled to the anodic and cathodic limits prior to addition of the compounds while no such cycling was performed with the gauze electrode.

(13) Robbins, J. L.; Edelstein, N.; Spencer, B.; Smart, J. C. *J. Am. Chem. Soc.* **1982**, *104*, 1882–1893 and references therein.

(14) For example, see: Manrigue, J. M.; McAlister, P. R.; Rosenburg, E.; Shiller, A. M.; Williamson, K. L.; Chan, S. I.; Bercaw, J. E. *J. Am. Chem. Soc.* **1978**, *100*, 3078–3083. McLain, S. J.; Wood, C. D.; Schrock, R. R. *Ibid.* **1979**, *101*, 4558–4570.

potentials and the stabilities of the $Fe(HB(pz)_3)_2$ couples are closer to those of $Fe(C_5Me_5)_2$ than to those of the $Fe(C_5H_5)_2$ couples.

Similarities are also evident in the d-orbital energy diagram for D_{5d} $Fe(C_5R_5)_2^+$ and D_{3d} $Fe(HB(pz)_3)_2^+$ shown in Figure 6. In both cases the separation, Δ, between the highest and second highest occupied orbitals is less than the spin-pairing energy.[13,15] This situation must prevail in the 2+ forms, at least for $Fe(C_5Me_5)_2^{2+}$, since the magnetic moment indicates a high-spin configuration. Thus, the first electron to be removed from the neutral complexes is from an a_{1g} orbital and the second is from an e_{2g} $Fe(C_5R_5)_2^+$ or a $1e_g$ $Fe(HB(pz)_3)_2^+$ orbital.

The absorption spectra of the 2+ complexes could yield data concerning orbital energy separations. However, as with other d^4 metallocenes, the band in the spectrum of $Fe(C_5Me_5)_2^{2+}$ centered at 430 nm is probably an unresolved juxtaposition of a number of spin-allowed transitions.[16] The spectrum of $Fe(HB(pz)_3)_2^{2+}$ is unusual in that the blue color of the complex is due to the tailoff of a strong band centered at 833 nm in the IR spectrum; a lower energy shoulder at 1080 nm is also present.

In conclusion, SO_2 has again proven to be a good solvent for electrochemical oxidations. This has allowed the observation of $Fe(C_5H_5)_2^{2+}$, another member of the large, but apparently still growing, group of transition-metal metallocenes, and the production of stable solutions of $Fe(C_5Me_5)_2^{2+}$ and $Fe(HB(pz)_3)_2^{2+}$.

Acknowledgment. Support of this research by the National Science Foundation (Grant CHE 7903729) is gratefully acknowledged.

Registry No. $1^+PF_6^-$, 11077-24-0; 1^{2+}, 86549-93-1; $2^+PF_6^-$, 54182-44-4; 2^{2+}, 75713-66-5; $3^+PF_6^-$, 86549-96-4; 3^{2+}, 86549-94-2; $Fe(C_5H_5)_2$, 102-54-5; $Fe(C_5Me_5)_2$, 12126-50-0; $Fe(HB(pz)_3)_2$, 16949-45-4; SO_2, 7446-09-5.

(15) Jesson, J. P.; Trofimenko, S.; Eaton, D. R. *J. Am. Chem. Soc.* **1967**, *89*, 3158-3164.

(16) Gordon, K. R.; Warren, K. D. *Inorg. Chem.* **1978**, *17*, 987-994.

Contribution from the Department of Chemistry, University of Pittsburgh, Pittsburgh, Pennsylvania 15260

Adjacent Methyl to Remote Methyl Isomerization of (4-Methylimidazole)pentaamminecobalt(III)[1]

M. FAZLUL HOQ, CRAIG R. JOHNSON, SUSAN PADEN, and REX E. SHEPHERD*

Received August 7, 1982

Isomers of (4-methylimidazole)pentaamminecobalt(III) have been isolated as chloride salts with the methyl group of the imidazole directed away from the five NH_3 ligands (remote = R) and near the NH_3 ligands (adjacent = Ad). Isomers have been assigned by a separate X-ray diffraction study. Isomers have been characterized by ^1H NMR spectra showing shifts (ppm) relative to the free ligand (L) as follows: 4-CH_3 Ad = 2.22, R = 2.33, L = 2.27; C_2-H Ad = 7.78, R = 7.88, L = 7.65; C_5-H Ad = 7.08, R = 6.73 (C_4-H), L = 6.77. In Tris or pyridinium buffers two paths are found for the isomerization of Ad to R. One path ($k_0 = (5.83 \pm 2.18) \times 10^{-8}$ s^{-1}) is attributed to the isomerization of the parent 4-methylimidazole species Ad. A second path, first order in [OD^-], is attributed to the imidazolato form Ad_{-H} ($k_{OH} = 3.19 \pm 0.07$ M^{-1} s^{-1}). The activation parameters for the k_{OH} path are $\Delta H^* = 32.4 \pm 4.1$ kcal/mol and $\Delta S^* = 16.8 \pm 11.7$ eu. A mechanism is presented, suggesting a largely dissociative-like transition state. Comparisons are made to the linkage isomerization of $(NH_3)_5Co^{3+}$ coordinated to ONO^- and N_1 of the 5-methyltetrazolato ligand. While the isomerization of the 5-methyltetrazole ligand is faster by 10^5 relative to that for 4-methylimidazole, the anion forms favor the 4-methylimidazolato isomerization by a factor of 400 vs. the 5-methyltetrazolato case. The difference is attributed to different basicity of the lone electron pairs of these ligands. The pK_a's of $(NH_3)_5CoX^{3+}$ have been found at 25.0 °C and $\mu = 0.10$ and are as follows (X, pK_a): imidazole, 9.99; 2-methylimidazole, 10.67; 4-methylimidazole (Ad), 10.46; 4-methylimidazole (R), 10.70. The acid dissociation constants of R and Ad were studied as a function of temperature, yielding values of $\Delta H°$, $\Delta S°$ as follows: (Ad) 17.7 ± 0.5 kcal/mol, 11.2 ± 1.6 eu; (R) 15.4 ± 0.6 kcal/mol, 2.5 ± 1.8 eu. The values of $\Delta H°$ are within a kilocalorie of imidazole's pyrrole pK_a (17.6 kcal/mol) while the values of $\Delta S°$ are more favored by charge dispersal for Ad and R by about 18 to 10 eu, respectively.

Introduction

Ellis and Purcell recently reported the preparation of (5-methyltetrazolato)pentaamminecobalt(III) by the addition of N_3^- across the triple bond of (acetonitrile)pentaamminecobalt(III)[2] as shown in Scheme I.

A slow isomerization ensues from N_1 to N_2 coordination as would be anticipated for removing the strain associated with the adjacent methyl group's interaction with cis-NH_3 ligands.[2,3] A 3.0-kcal strain energy has been calculated from association constants of imidazole and 4,5-dimethylimidazole for $Fe(CN)_5^{3-}$, where ligand repulsions ought to be of similar magnitude.[3] Linkage isomerization reactions between donor atoms of the same kind are much more rare than those between different atoms as in NCS^-, NO_2^-, CN^-, etc., where electronegativity and structural factors provide a driving force for

Scheme I

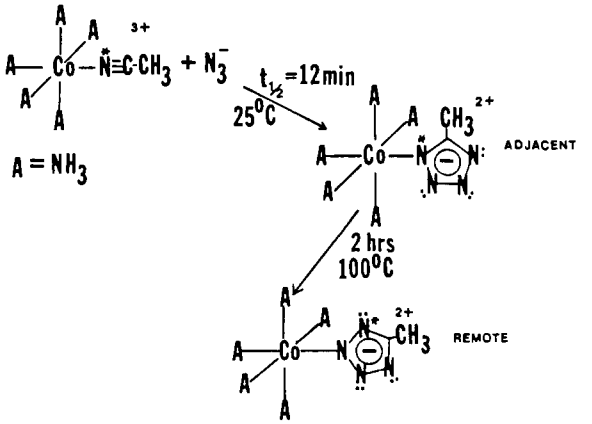

(1) A preliminary report was presented at the 183rd National Meeting of the American Chemical Society, Las Vegas, NV, April 1982.
(2) Ellis, W. R.; Purcell, W. L. *Inorg. Chem.* **1982**, *21*, 834.
(3) Shepherd, R. E. *J. Am. Chem. Soc.* **1976**, *98*, 3329.

0020-1669/83/1322-2693$01.50/0